Chapter 28
Zinc Oxide and Its Applications

Shun Hsyung Chang, Chih Chin Yang, Ting-hao Hu, Shang yang Chen and Ian Yi-yu Bu

Over the past decades, there have been intensive interests in research on zinc oxide (ZnO). The high electron mobility, high thermal conductivity, wide and direct band gap and large exciton binding energy make ZnO suitable for a wide range of devices, including transparent thin-film transistors, photodetectors, light-emitting diodes and laser diodes that operate in the blue and ultraviolet region of the spectrum. In spite of the recent rapid developments, controlling the electrical conductivity of ZnO has remained a major challenge. While a number of research groups have reported achieving *p*-type ZnO, there are still problems concerning the reproducibility of the results and the stability of the *p*-type conductivity. Even the cause of the commonly observed unintentional *n*-type conductivity in as-grown ZnO is still under debate. In this paper, we will present some of the work on ZnO from our laboratory.

28.1 Introduction

Zinc oxide is an important material for semiconductor applications. It possesses a direct wide band gap 3.37 eV and large free-exciton binding energy 60 meV [1, 2]. Generally, as deposited ZnO shows *n*-type conduction behaviour due to its structure defects and incorporated impurities [3]. Although such *n*-type behaviour has been explored in various optoelectronic applications it presents serious obstacles in its usage in semiconductor industry [4–6]. In other word, the use of ZnO as a semiconductor in electronic devices has been hindered by the difficulty in obtaining stable *p*-type ZnO. So far, two strategies have been developed to synthesis *p*-type ZnO: (i) direct doping through substituting group V elements such as N [7], P [8] or As [9] for O, and (ii) co-doping of N or Li acceptor with reactive

S. H. Chang · C. C. Yang · T. Hu · S. y. Chen · I. Y. Bu (✉)
Department of Microelectronics Engineering, National Kaohsiung Marine University, Kaohsiung, Republic of China (Taiwan)
e-mail: ianbu@webmail.nkmu.edu.tw

S.-H. Chang et al. (eds.), *Advanced Materials*, Springer Proceedings in Physics 152,
DOI: 10.1007/978-3-319-03749-3_28,

donors such as Ga, In or Al [10, 11]. The N/Al combination is preferred due to material abundance and the greater acceptance by the semiconductor manufacturers.

Another emerging research area of ZnO is reducing its dimensions into nanometer scale. Different geometries of ZnO nanomaterials such as, nanowires [12] nanoplates [13], nanoflake [14] and nanoflower [15] have been obtained. ZnO is suitable material for humidity sensor as its resistivity is sensitive to changes in humidity due to adsorption of hydrogen gas molecules [14]. The desired characteristics of a high performance moisture sensor include fast response, high sensitivity, durable and cost effective. It is expected that by adapting ZnO into nanomaterials can offer further enhancement in moisture sensitivity due to increased surface area.

In this paper, we will introduce the latest work on ZnO from National Kaohsiung Marine University.

28.2 Sol–Gel Deposition of *p*-Type ZnO Through Co-doping Method

Sol–gel deposition of *p*-type ZnO : Al : N was obtained by stirring 0.7 M zinc acetate ($Zn(CH_3COO)_2{\cdot}H_2O$) in isopropanol IPA, with an 0.7 M of MEA added as a chelating agent to prevent precipitation. The solution was magnetically mixed at 70° C for 1 h until a transparent solution was formed. NH_4Cl (0.03 M) and NH_4OH were selected as the nitrogen source and the co-doping was achieved by adding 1 wt% $AlCl_3$ into the precursor solution. For comparison purposes, a sample without Al co-doping was also synthesized. Depositions were achieved in atmospheric air using a spin coater set at 3000 rpm for 30 s. The deposited thin films were first heated to 250° C, in order to evaporate the solvents, and subsequently sintered to 550° C by a hotplate to crystallize the films.

Figure 28.1 shows SEM image of surface morphology of the NZO films doped with different nitrogen source [1]. Figure 28.1a, b show NZO produced via sol–gel method consists of a wrinkled thin film embedded within smaller grain ZnO particles. Both the films exhibit wrinkle-network on the surfaces. Such "wrinkle" effects have been observed in the past and is usually attributed to stress relaxation during the cooling of the ZnO thin film. The wrinkle effect is only visible on at lower magnification (5 mm scale) (see Fig. 28.1a). Figure 28.1b–d show SEM of the films at higher resolution. The NZO films on glass composed of compact and dense nanoparticles with diameters of 10–50 nm. The grain size of ZnO films are affected by the post annealing temperature. Typically, as the temperature increases the density and grain size of ZnO increase. The *c*-axis oriented and dense packed structure is typical of the films deposited by sol–gel method.

Figure 28.2 shows the XRD patterns of the deposited NZO films. All the films showed preference growth along the (002) plane. The quality of the XRD peaks is

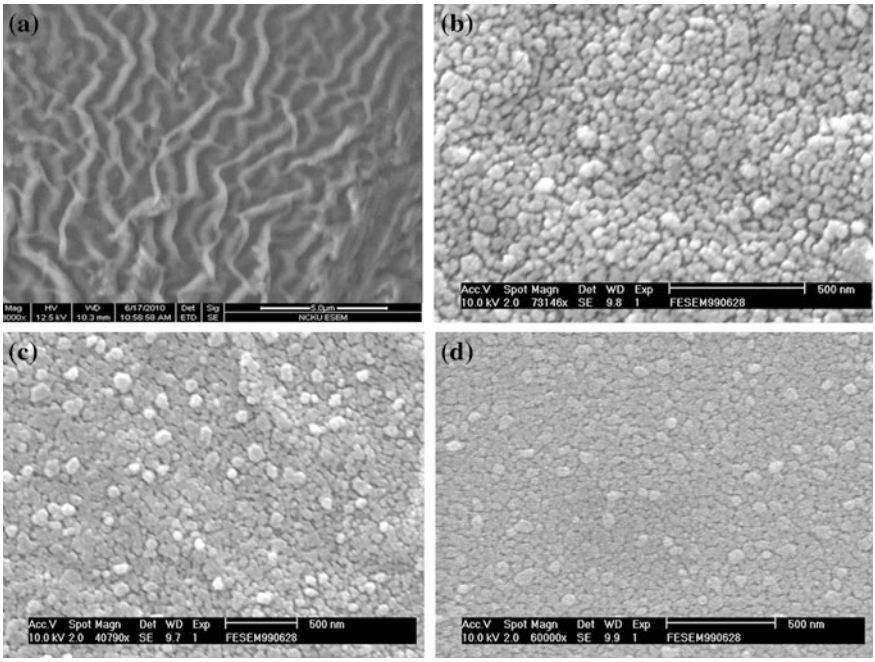

Fig. 28.1 SEM image: **a** typical sol–gel derived NZO film at lower magnification, **b** sol–gel synthesized NZO without Al co-doping, **c** sol–gel produced ZnO : Al : N using NH_4Cl as source of nitrogen, **d** sol–gel produced ZnO : Al : N using NH_4OH as source

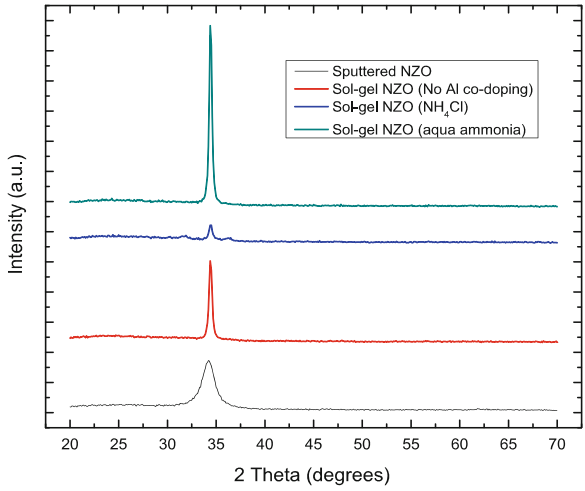

Fig. 28.2 XRD of the synthesized NZO films, sol–gel synthesised AZO, sol–gel produced ZnO : Al : N using NH_4Cl as source of nitrogen, sol–gel produced ZnO : Al : N using NH_4OH as source and sputtered ZnO : Al : N [1]

an indication of the degree of crystallinity. As expected, the sputtered ZnO : Al : N showed a broad peak which indicates the amorphous structure of the film. Figure 28.2 illustrates that the XRD pattern for ZnO : Al : N is very sensitive to chemical selection. The films, derived from NH_4Cl, produced weaker XRD signal intensity than NH_4OH. The results are significant and indicate the orientation and quality of *p*-type ZnO films that can be controlled through chemistry of the sol. The utilisation of NH_4OH produced high quality crystalline film with extreme preference to *c*-axis. The Hall measurement confirms *p*-type conductivity of the films. *P*-type properties of sol–gel processed ZnO films are highly dependent on nitrogen source. Without co-doping we can observe film with high resistivity. Films co-doped with aluminium all have acceptable resistivity with hole concentration in the 10^{17} cm^{-3} and resistivity range between 45–62 cm^2/Vs.

28.3 Effect of NH_4OH Concentration on *P*-Type Doped Zinc Oxide Film by Solution Based Process

In subsequent study, we investigated the effect of ammonia concentration on optoelectronic properties of *p*-type ZnO : Al : N [4]. Figure 28.3 shows the surface morphology of the films obtained via spin coating of the sol precursor solution with different NH_4OH concentration. In Fig. 28.2, it can be observed from insets of the SEM images, that the calcinated film consists of NZO nanoparticles of around 30–50 nm. Films with 1 ml NH_4OH exhibit smooth surface. As the concentration of NH_4OH increases to 2.5 ml, small patches of agglomerate appeared. This trend continues, as further increase of NH_4OH to 5 ml, yield films with more prevalent agglomeration. The data suggest excessive NH_4OH leads to agglomeration formation in NZO films. The mechanism of agglomeration is discussed at a latter section of this article.

Figure 28.4 shows the crystal orientation of the sol–gel derived NZO films with different concentration of NH_4OH. The results of these films showed preferential orientation towards (002) orientation. The preferred orientation decreases with increasing NH_4OH addition. With the addition of 5 ml of NH_4OH into the precursor, the resultant film consists of crystallites with random orientation. It is well known, that the orientation of the crystallites is strongly dependant on the chemistry of the precursor. The random orientated crystallites synthesized at 5 ml NH_4OH suggest the possibility of other phases, such as AlN or Zn_3N_2 in the doped film. The XRD data correlates the corresponding SEM image where random agglomeration can be clearly seem within the film.

Hall effect measurements for NZO films were measured by the four-probe van der Pauw method. Data were averaged to ensure accuracy. All the films show *p*-type conduction, indicate N incorporation via Al co-doping. Figure 28.5 shows the resistivity as a function of NH_4OH concentration. It can be observed that, when NH_4OH is introduced to the sol, resistivity of *p*-type ZnO film is reduced. The minimum resistivity as determined by Hall measurements occurs at around 2.5 ml

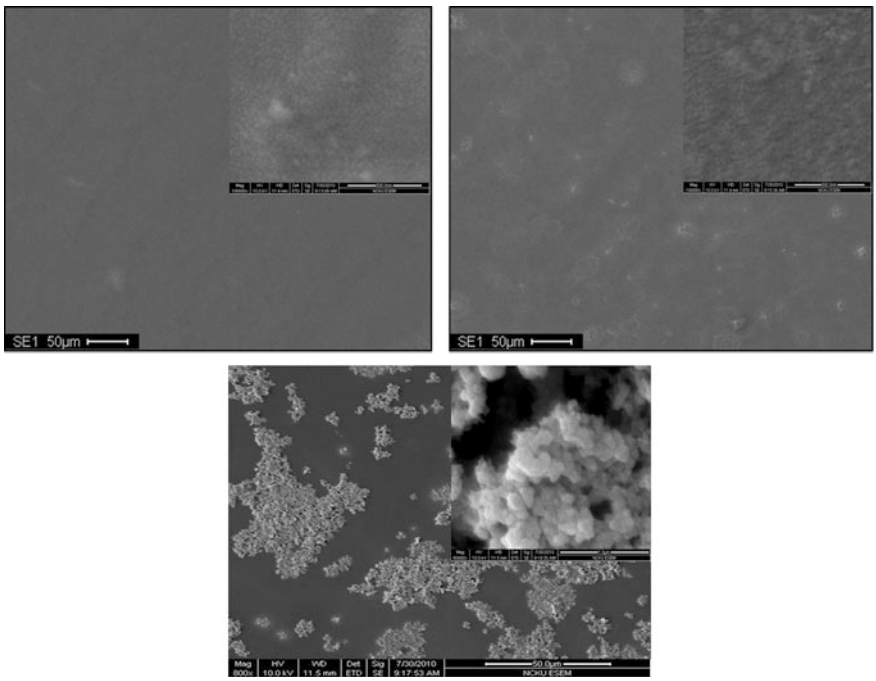

Fig. 28.3 Effect of ammonia concentration on the structure of *p*-type ZnO

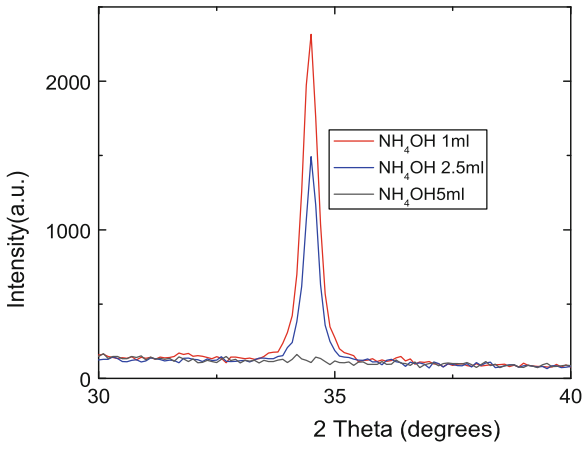

Fig. 28.4 Crystal orientation of the sol–gel derived NZO films with different concentration of NH_4OH

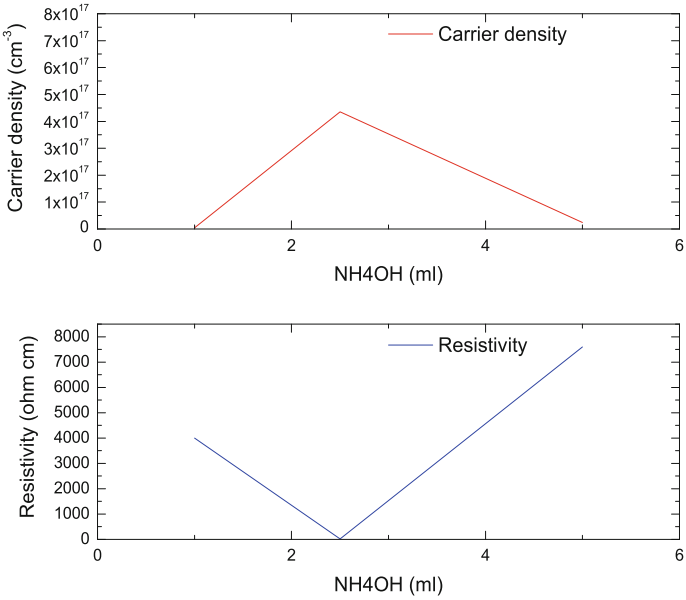

Fig. 28.5 Hall effect measurements for NZO films were measured by the four-probe van der Pauw method

of NH_4OH. Further increase in NH_4OH concentration resulted in films with higher resistivity. As NH_4OH concentration increases, the hole concentration increases and resistivity decreases. The increase of hole concentration is due to an increase in the quantity of N molecules due to an increase in the concentration of NH_3 molecules dissociated into N and NO molecules with an increase of NH_4OH. Further increase of NH_4OH (5 ml), resulted in precipitates in the films, which act as a defect and scattering centers, degrades the carrier mobility and increases resistivity.

Excessive NH_4OH concentration results in a large density of oxygen vacancies and zinc interstitials will exist in ZnO crystal due to the absence of oxygen in ambient acting as donors. Therefore, the carrier density of *p*-type ZnO is reduced greatly because of high self compensation. The NH_4OH shifts the PH of the solution towards alkaline deposition, which results in accelerated rate of condensation than hydrolysis. This favors agglomeration of larger particles. The incorporation of excessive nitrogen alters the structure and affects its electrical property.

28.4 Conclusion

In this study, *p*-type ZnO was successfully deposited using sol–gel deposition method. It was found that the ammonia concentration has a profound effect on its subsequent structure and optoelectronic properties.

References

1. I.Y. Bu, J. Alloy. Compd. **509**(6), 2874 (2011)
2. C.F. Klingshirn, *Zinc Oxide: From Fundamental Properties Towards Novel Applications* (Springer, Berlin, 2010)
3. A. Janotti, C.G. Van de Walle, Rep. Prog. Phys. **72**(12), 126501 (2009)
4. I.Y. Bu, Appl. Surf. Sci. **257**(14), 6107 (2011)
5. I.Y. Bu, Ceram. Int. **39**(5), 1189–1194 (2013)
6. I.Y. Bu, Superlattices Microstruct. **64**(4), 213–219 (2013)
7. A. Tsukazaki, A. Ohtomo, T. Onuma, M. Ohtani, T. Makino, M. Sumiya, K. Ohtani, S.F. Chichibu, S. Fuke, Y. Segawa, Nature Mater. **4**(1), 42 (2004)
8. K.–K. Kim, H.-S. Kim, D.-K. Hwang, J.-H. Lim, S.-J. Park, Appl. Phys. Lett. **83**(1), 63 (2003)
9. A. Dadgar, A. Krtschil, F. Bertram, S. Giemsch, T. Hempel, P. Veit, A. Diez, N. Oleynik, R. Clos, J. Christen, Superlattices Microstruct. **38**(4), 245 (2005)
10. J. Lu, Z. Ye, F. Zhuge, Y. Zeng, B. Zhao, L. Zhu, Appl. Phys. Lett. **85**(15), 3134 (2004)
11. F. Zhuge, L. Zhu, Z. Ye, D. Ma, J. Lu, J. Huang, F. Wang, Z. Ji, S. Zhang, Appl. Phys. Lett. **87**(9), 092103 (2005)
12. I.Y. Bu, Ceram. Int. **38**(12), 3869–3873 (2012)
13. Y. Qiu, W. Chen, S. Yang, J. Mater. Chem. **20**(5), 1001 (2010)
14. I.Y. Bu, C.–C. Yang, Superlattices Microstruct. **51**(6), 745 (2012)
15. L.–L. Xing, C.-H. Ma, Z.-H. Chen, Y.-J. Chen, X.-Y. Xue, Nanotechnology **22**(21), 215501 (2011)